Mechanics of Materials 16 (1993) 179–187
Elsevier

On the structure of three-dimensional shear flows

M.A. Hopkins [a], J.T. Jenkins [b], and M.Y. Louge [c]

[a] *US Army Cold Regions Research and Engineering Laboratory, Hanover, NH 03755-1290, USA*
[b] *Department of Theoretical and Applied Mechanics, Cornell University, Ithaca, NY 14853, USA*
[c] *Sibley School of Mechanical and Aerospace Engineering, Cornell University, Ithaca, NY 14853, USA*

Received 16 April 1992; accepted 18 August 1992

This paper describes an investigation of structure in moderately dilute three-dimensional shear flows. Structure is defined as a dynamic inhomogeneity or fluctuation in the spatial concentration field.

Numerical experiments are performed with large numbers of identical, frictionless, inelastic spheres. The spheres are contained in a fully periodic cubic control volume. A state of shear is maintained in the control volume by moving the upper periodic image in one direction and the lower image in the opposite direction. As the coefficient of restitution of the spheres is lowered, conditions in the control volume deviate from a state of simple shear, exhibiting strong wavelike fluctuations in the concentration, stress, and velocity fields. Visual inspection of the spatial concentration field reveals a strong tendency for spheres with a low coefficient of restitution to form dense elongated clouds. The major axis of the clouds tends to align itself in the direction of the mean velocity and perpendicular to the direction of variation in the mean velocity created by the moving periodic images of the control volume.

Introduction

A granular material is an aggregate of discrete solid particles. Rapid flows of granular materials occur in geophysical phenomena such as rock slides, debris flows, and snow avalanches, in the motion of the marginal ice zones surrounding the central Arctic ice pack, and in industrial processes involving the bulk transport of coal, grain, and powders.

Early theoretical treatments of granular flows (Jenkins and Savage, 1983; Lun et al., 1984) following from the kinetic theory of dense gases (Chapman and Cowling, 1970) were limited to nearly elastic flows by their assumption of a Maxwellian velocity distribution. Recently, Jenkins and Richman (1988) and Chou (1990) have developed theories for more inelastic flows using a joint Maxwellian distribution, by explicitly treating the anisotropy of the second moment of the velocity fluctuations. However, both theories retain the assumption of molecular chaos, the cornerstone of the kinetic theory. Implicit in the chaos assumption is the assumption that the spatial distribution of particles is locally isotropic and homogeneous.

Campbell (1986) observed the formation of a distinct layered structure in particle simulations of very dense shear flows. In two-dimensional simulations of dilute shear flows using uniform disks, Hopkins and Louge (1991) observed a dynamic micro-structure caused by inelastic collisions. This inelastic micro-structure was characterized by dynamic clusters of disks on the order of 10 diameters in size. Because many such clusters were distributed throughout a control volume (see Fig. 1), shear flows of low to medium density may still be homogeneous on scales of many particle diameters. Walton et al. (1991) reported large variations in normal stress ratios in simula-

Correspondence to: Dr. M.A. Hopkins, US Army Cold Regions Research and Engineering Laboratory, Hanover, NH 03755-1290, USA.

tions of dilute shear flows, with large numbers of highly inelastic spheres, which were attributed to micro-structure.

In the present work, structure in dilute three-dimensional shear flows of identical, frictionless spheres is investigated. The results of this study differ radically from the results reported by Hopkins and Louge for two-dimensional shear flows of disks.

2. The particle simulation method

The numerical experiments are performed using a particle simulation method described in detail by Hopkins and Louge (1991). In this method, the cubic control volume (CV) of length L is periodic in all three directions. A sphere that leaves one face simultaneously re-enters the CV through the opposite face. A state of shear is maintained in the CV by moving the upper and lower periodic images of the CV in opposite directions. In this work, the moving images of the CV lie in the y-direction with mean velocities in the x-direction in a coordinate frame aligned with the edges of the cubic CV. After each time step, the position of each sphere is calculated from its previous position and velocity. Collisions occur when one sphere slightly overlaps a neighbor. The average overlap in the experiments was

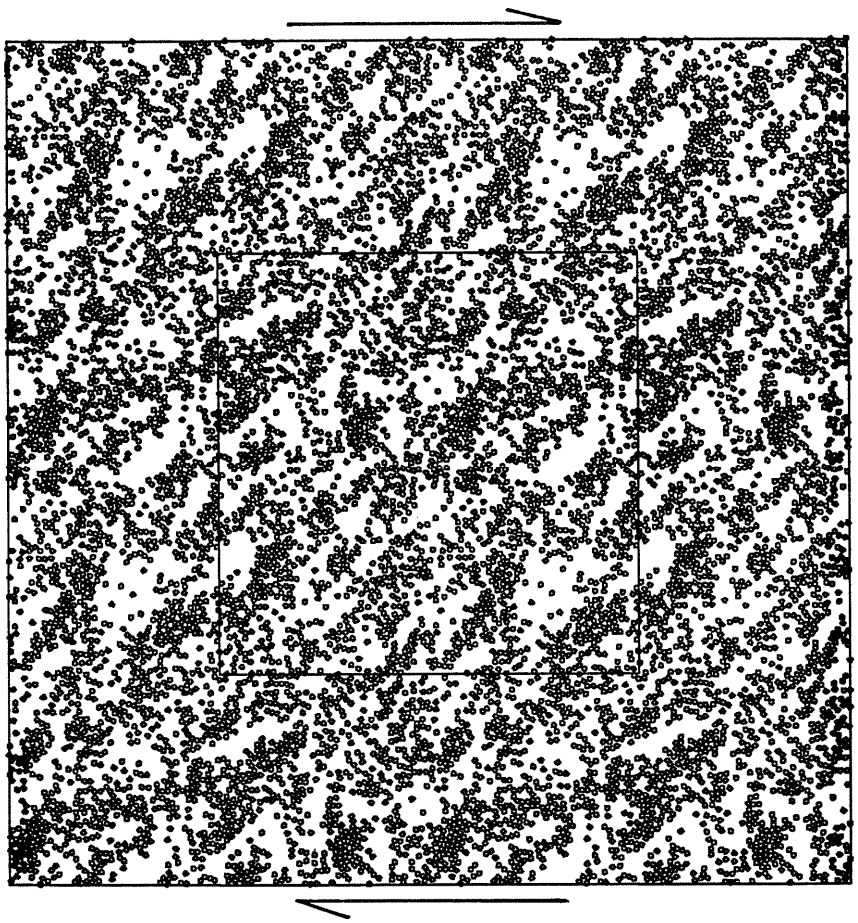

Fig. 1. The distribution of disks in a two-dimensional shear flow for the conditions $\nu = 0.3$, $L/d = 83$, and $e = 0.2$. The square bounds the periodic control volume of the simulation and the arrows represent the direction of shear (from Hopkins and Louge, 1991).

held to 1.5% of the sphere diameter d by regularly re-adjusting the simulation time step. The post-collision velocities are calculated by balancing linear momentum before and after the collision and using a coefficient of restitution e to characterize the incomplete restitution of relative translational velocity in the direction parallel to the line connecting the particle centers.

To begin the simulation, the spheres are placed in a cubic array. They are given an initial velocity proportional to their y-coordinate and to an assumed linear mean velocity gradient between the top and bottom periodic images. They are also given a small, random velocity component. The total initial momentum of the system is zero in all directions. The center of mass lies at the center of the CV and the spheres are evenly distributed in space. The mean velocity of the upper periodic image of the CV with respect to the lower image is $U = 1.0$ in the x-direction. The unit of length in the experiments is the width of the CV and the unit of time is one second. The simulations were run in double precision and no significant momentum imbalance was detected after any experiment.

3. The variance of the concentration field

Hopkins and Louge used a two-dimensional Fourier transform of the spatial concentration field to characterize structure in a rapidly sheared system of inelastic disks. Unfortunately, the Fourier transform is a very expensive method, computationally, with which to measure the structure of three-dimensional concentration fields.

An alternative method used by Sanders and Ackermann (1991) is to divide the CV into uniform cells, count the number of particle centers in each cell, and calculate the average variance of the concentration field. In the following experiments, the CV is divided into a $10 \times 10 \times 10$ array of cubic cells. The variance of the concentration field, for a given realization of the system, is

$$\text{variance} = (1/1000) \sum_i (n_i - N/1000)^2, \qquad (1)$$

where Σ_i is a sum over the cells, n_i is the number of sphere centers in cell i and N is the total number of spheres in the CV. A series of experiments was performed with 6859 (19^3) spheres, in

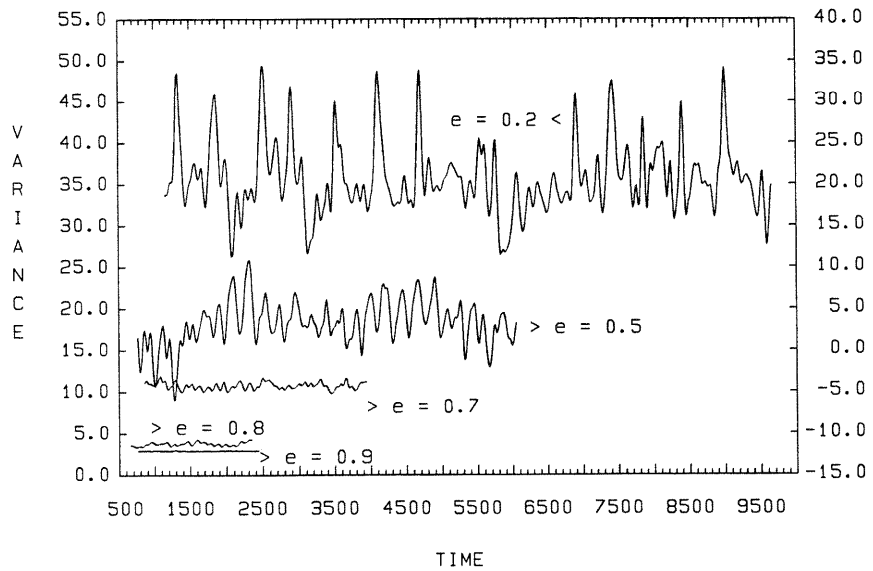

Fig. 2. Plots of variance (1) versus time for the conditions $\nu = 0.2$, $L/d = 26$. The scale for $e = 0.2$ is on the right and the scale for $e > 0.2$ is on the left. The data was smoothed using a low pass filter with a cut-off frequency of 0.01 s^{-1}.

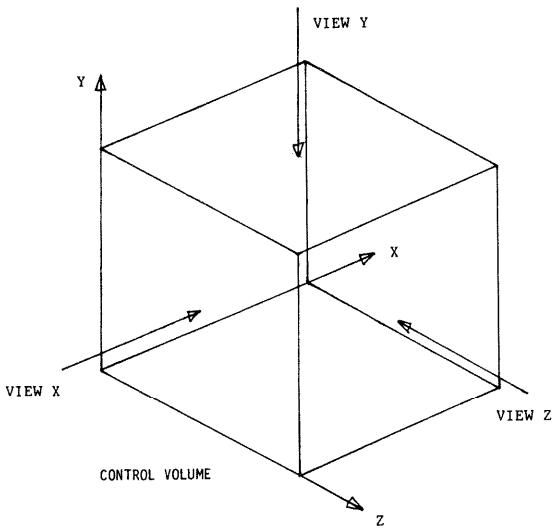

Fig. 3. Orientations for viewing slices of the three-dimensional control volume.

which the coefficient of restitution e was reduced from 0.9 to 0.2. The solid fraction ν was 0.2 and $L/d = 26$. Figure 2 shows the variance (1) versus time for several values of e. The data were smoothed using a low pass filter with a cut-off frequency of 0.01 s^{-1}. The plot shows that as e decreases both the mean value of the variance and the size of the fluctuations in the variance increase.

The variance of the concentration field, measured over a grid of cells in which the average number of spheres per cell is 6.859, is not a direct measure of large-scale structure in the CV. To see how the variance correlates with large-scale structure, the spatial concentration fields were visually compared during periods of high and low variance. Three-dimensional snapshots of the concentration field conceal voids and regions of high density. Therefore, cross-sections of the concentration field are used to reveal three-dimensional structure. The CV is sliced into 40 cross-sections of equal thickness in each of the three coordinate directions, that is, normal to each axis. The average number of sphere centers in each slice is 171. Figure 3 shows the viewpoints for the slices.

Figure 4 shows the concentration field at 2100 s with $\nu = 0.2$, $e = 0.2$, and $L/d = 26$ during a period of low variance in Fig. 2. Seven of the 40 slices in each of the three directions are arranged in three strips corresponding to views in the x- (top strip), y- (middle), and z- (bottom) direc-

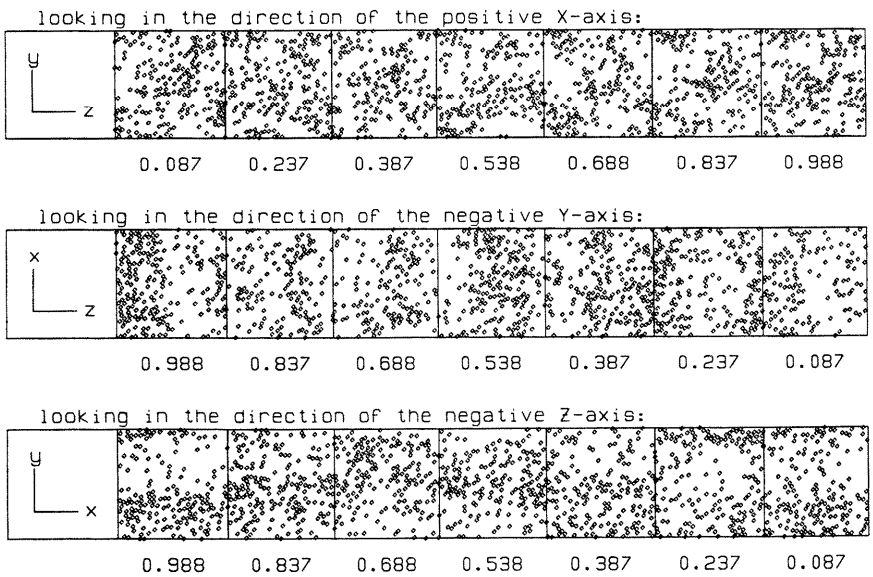

Fig. 4. Slices of the three-dimensional control volume in each of the three coordinate directions at time = 2100 s for the conditions $\nu = 0.2$, $e = 0.2$, $L/d = 26$.

tions. The number beneath each slice gives the distance of the slice from the origin measured along the axis parallel to the viewing direction. Although the concentration field is not homogeneous, there is no well defined structure.

Figure 5 shows the concentration field, at 2500 s of the same experiment, during the following period of high variance in Fig. 2. The slices show two large cloudlike structures of high density surrounded by very dilute regions. The slices in the top strip, views of the CV looking in the x-direction, show little variation. The second and third strips show views of the CV looking in the y- and z-directions, respectively. The structure shown in both strips is parallel to the x-direction. Interestingly, there is no evidence of the characteristic diagonal structure seen in similar two-dimensional shear flows of identical disks by Hopkins and Louge (see fig. 1). The diagonal structure was caused by rotation and stretching of clusters by the mean shear field. Examination of other times of high and low variance in Fig. 2 shows a similar qualitative agreement with the structure of the concentration field in visualizations of the CV.

4. The probability density of the concentration field

A smooth spatial concentration field is created (Hopkins and Louge, 1991) by dividing the CV into cubic cells. The cells have a dimensionless width $a = w/d$, where w is the cell width and d is the sphere diameter. In the present experiments $a = 0.92/\sqrt{2}$. Each cell may contain no more than one sphere center. The volume of each sphere is assigned to the cell in the three-dimensional grid in which its center lies. This produces a binary concentration field in which a cell either contains a sphere or it does not. Therefore, the concentration field is smoothed using a low pass filter with a transition frequency of $1/12a$. The smoothing filter has the effect of distributing the volume of each sphere over its immediate neighborhood. Since the neighborhood is small com-

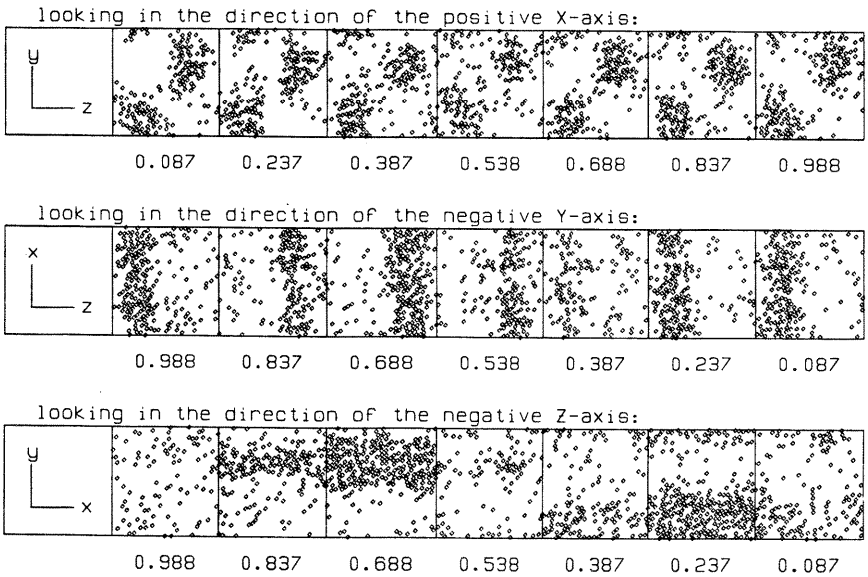

Fig. 5. Slices of the three-dimensional control volume in each of the three coordinate directions at time = 2500 s for the conditions $\nu = 0.2$, $e = 0.2$, $L/d = 26$.

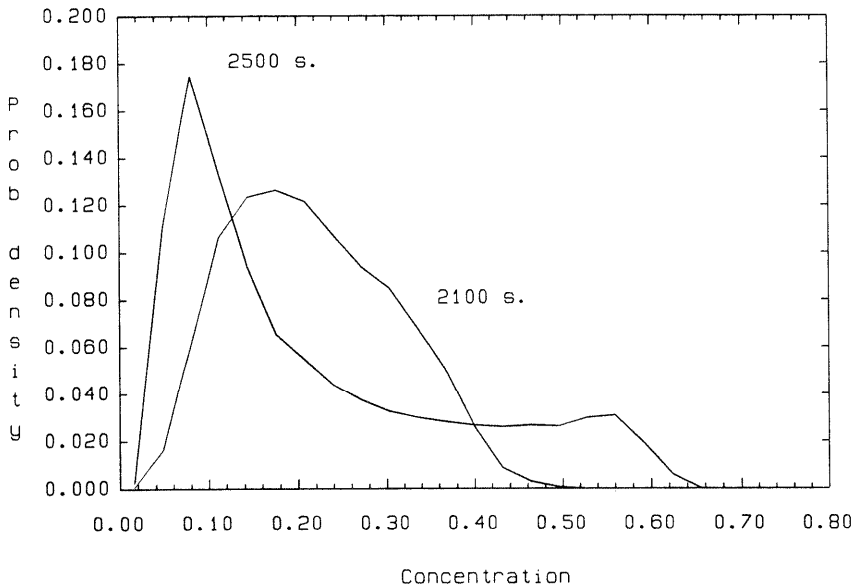

Fig. 6. The probability density function of the concentration fields shown in Figs. 5 and 6, comparing times of low (2100 s) and high (2500 s) structure.

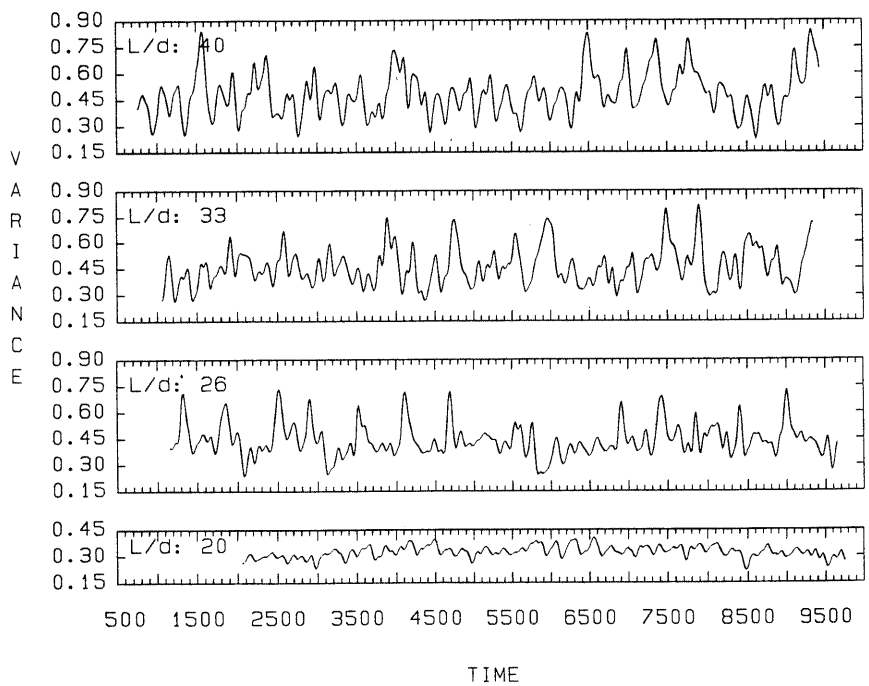

Fig. 7. Plots of variance (1) versus time for the conditions $\nu = 0.2$, $e = 0.2$. The variances are normalized by the square of the average number of spheres per cell in each experiment. The data were smoothed using a low pass filter with a cut-off frequency of 0.01 s^{-1}.

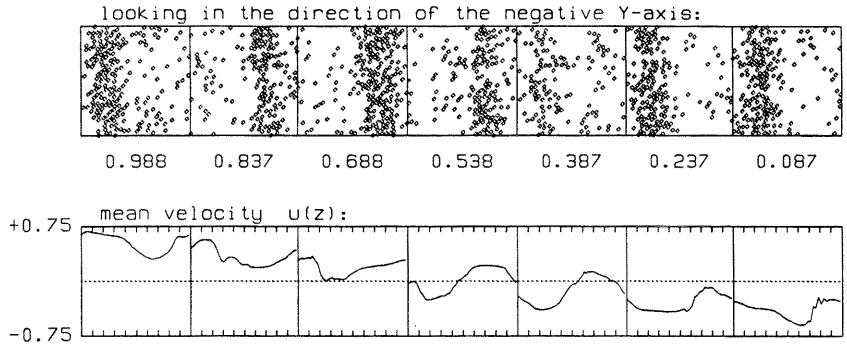

Fig. 8. The gradient of the mean velocity $u(z)$ for the cross-sections shown in Fig. 5, looking in the direction of the negative y-axis. (Refer to Fig. 5 for the coordinate directions in the lower strip.)

pared to the CV, the local concentration field is accurately represented. The smoothing function is $g(p, q, r)$:

$$g(p, q, r) = \sin c(p/6) \sin c(q/6) \sin c(r/6) \times \left(\sum_p \sum_q \sum_r \sin c(p/6) \times \sin c(q/6) \sin c(r/6) \right)^{-1}, \quad (2)$$

where the integers p, q and r correspond to the x-, y-, and z-directions, $\sin c(x) = \sin(\pi x)/\pi x$, and the summations are performed from -5 to $+5$, that is, on the $11 \times 11 \times 11$ cell region surrounding the cell in which the sphere's center is located.

The probability density of the concentration field is shown in Fig. 6 for the two realizations whose cross-sections are shown in Figs. 4 and 5. The mean concentration was $\nu = 0.2$. The two realizations show qualitatively different distributions of particle concentration. The distribution at 2100 s corresponds to a period of low variance. At 2500 s, in a period of high variance, the distribution is nearly bimodal, with large areas of dilute concentration and areas of high density approaching random solid packing.

5. The dependence of the variance on number density

The dependence of the variance of the concentration field on the number of spheres in the unit

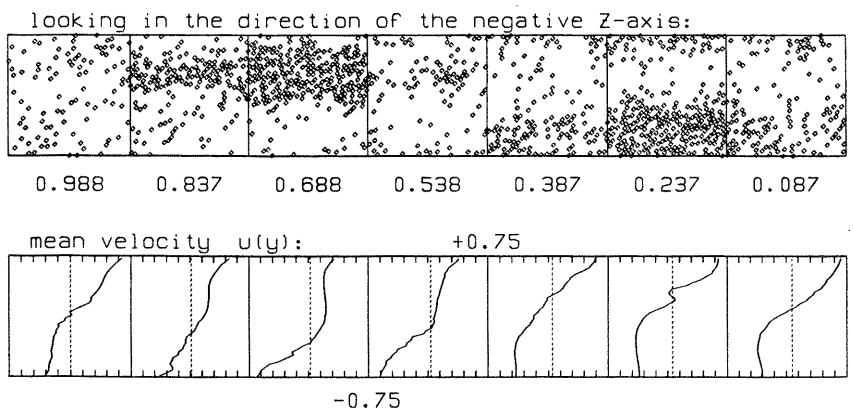

Fig. 9. The gradient of the mean velocity $u(y)$ for the cross-sections shown in Fig. 5, looking in the direction of the negative z-axis. (Refer to Fig. 5 for the coordinate directions in the lower strip.)

CV was examined by performing experiments with $\nu = 0.2$ and $e = 0.2$ for ratios of L/d of 20, 33, and 40. The plots of variance versus time obtained in these experiments are compared in Fig. 7 with the variance at L/d of 26 shown in Fig. 2. The variances in Fig. 7 are normalized by the square of the average number of spheres per cell in each experiment. The experiment at $L/d = 20$ used an $8 \times 8 \times 8$ array of cells, while the remainder used a $10 \times 10 \times 10$ array. The mean/variance of the plotted variances for L/d of 20, 26, 33, and 40 are, respectively, 0.323/0.001, 0.440/0.008, 0.460/0.011, and 0.483/0.015. Although the time series appear periodic, their Fourier power spectrums do not exhibit clear peaks.

6. Mean velocity gradients

The mean velocity field in the CV is maintained by the relative motion of the upper (in the y-direction) periodic image of the CV with respect to the lower image. In a simulation with nearly elastic spheres, the mean velocity gradient is approximately linear, even when averaged over small time intervals. However, because of the effects of particle clouds, the gradients in the inelastic shear flows studied here are highly nonlinear. Figure 8 shows the variation in the mean of the x-component of velocity $u(z)$, in each of the cross-sections in Fig. 5, looking in the direction of the y-axis. Figure 9 shows the variation in the mean of the x-component of velocity $u(y)$, in each of the cross-sections in Fig. 5, looking in the direction of the z-axis. In Figs. 8 and 9 the mean velocity profile in each cross-section is plotted on a scale of -0.75 to $+0.75$. In a homogeneous simple shear flow, the mean velocity $u(z)$ in Fig. 8 would be zero and the mean velocity $u(y)$ in Fig. 9 would be linear from -0.5 to $+0.5$. In both figures, the mean velocity profile shows large variation in the z-direction and the mean velocity gradient through the clouds is nearly flat.

7. The granular temperature field

The fluctuating velocity field, defined in terms of the local mean velocities, defines the granular temperature field. Intuitively, one expects spheres in the dense regions in Fig. 5 to have a lower granular temperature (smaller velocity fluctuations) than spheres in the surrounding dilute regions. The granular temperature field in a cross-section can be found by first calculating the smoothed concentration field in the CV using the method described above.

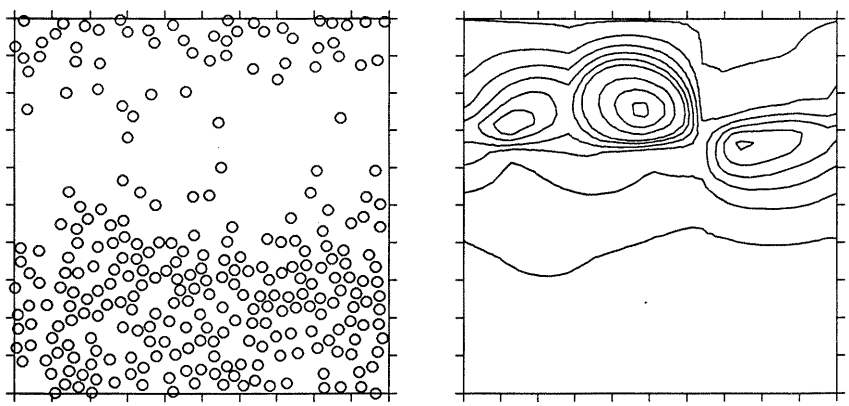

Fig. 10. The smoothed granular temperature field for the cross-section at $z = 0.237$ in the bottom row in Fig. 5. The densely contoured areas of the figure denote areas of relatively high temperature.

The granular temperature field is calculated in a similar manner. The fluctuating kinetic energy (ke) of a sphere k

$$\mathrm{ke}_k = (u_k - \langle u \rangle_j)^2 + (v_k)^2 + (w_k)^2, \qquad (3)$$

is assigned to the cell in which its center lies. The symbols u, v, w denote velocity components in the x-, y-, and z-directions. The mean velocity $\langle u \rangle$ is averaged over strips normal to the y-direction as in Fig. 9. The granular temperature field is smoothed using (2). The value of the smoothed temperature field in a cell is divided by the value of the smoothed concentration field in the cell to obtain the specific temperature field. The specific temperature field shows the temperature of the spheres in a region rather than the total energy contained in the region. Figure 10 shows, qualitatively, the specific granular temperature field for the cross-section at $z = 0.237$ in the bottom row in Fig. 5 using the corresponding mean velocity gradient in Fig. 9. The densely contoured areas of the figure denote temperature peaks in the dilute region.

8. Conclusion

In this work, the structure of three-dimensional shear flows was investigated. The variance of the concentration field on a medium scale between the length of the control volume L and the sphere diameter d was used to describe the time history of structure formation and disintegration. The periods of high and low variance were found to correlate with structure shown in cross-sectional snapshots of the simulation. The size of the fluctuations in the variance was shown to depend on the coefficient of restitution e and on the ratio L/d. Dependence on the solid fraction ν was not investigated.

The mean velocity gradient was shown to be highly non-linear. The presence of particle clouds caused variations in mean velocity in the transverse (z) direction as well as in the direction (y) of the imposed shear. The granular temperature in cross-sections calculated using the local mean velocity was qualitatively investigated and found to be much higher in the dilute regions surrounding the clouds than in the clouds themselves.

Traditionally, fully periodic simulations have been performed to determine the effects of variations in important parameters such as solid fraction ν, restitution e, and friction μ on the stresses in the CV. In these simulations, with relatively small numbers of particles, deviations from simple shear occur over very short periods relative to the duration of the simulation. In the experiments reported here, using much larger systems of particles, profound deviations from simple shear are observed to persist for long periods.

The diagonally periodic structure (see Fig. 1) composed of relatively small clusters of particles, which dominated the two-dimensional flows investigated by Hopkins and Louge (1991), was not observed in cross-sectional snapshots of the three-dimensional shear flows.

References

Campbell, C.S. (1986), The effect of microstructure development on the collisional stress tensor in a granular flow, *Acta Mech. 63*, 61–72.

Chapman, S. and T.G. Cowling (1970), *The Mathematical Theory of Non-Uniform Gases*, Cambridge University Press, Cambridge, 3rd edn.

Chou, C.S. (1990), Boundary effects, grainsize reduction, and normal stress differences in rapid granular flow, Ph.d. Dissertation, Worcester Polytechnic Institute.

Hopkins, M.A. and M.Y. Louge (1991), Inelastic micro-structure in rapid granular flows of smooth disks, *Phys. Fluids A 3(1)*, 47–57.

Jenkins, J.T. and S.B. Savage (1983), A theory for the rapid flow of identical, smooth, nearly elastic, spherical particles, *J. Fluid Mech. 130*, 187–202.

Jenkins, J.T. and M.W. Richman (1988), Plane simple shear of smooth, inelastic circular disks: The anisotropy of the fluctuation energy in the dilute and dense limits, *J. Fluid Mech. 192*, 313–328.

Lun, C.K.K., S.B. Savage, D.J. Jeffrey and N. Chepurniy (1984), Kinetic theories for granular flow: Inelastic particles in a Couette flow and slightly inelastic particles in a general flow field, *J. Fluid Mech. 140*, 223–256.

Sanders, B.E. and N.L. Ackermann (1991), Instability in granular chute flows, *J. Eng. Mech. ASCE 117*, 2396–2406.

Walton, O.R., H. Kim, and A.D. Rosato (1991), Microstructure and stress differences in shearing flows, in: *Mechanics Computing in 1990's and Beyond, (Proc. ASCE Engineering Mechanics Specialty Conference)*, Columbus OH, May 20–22, 1991.